

# A Non-Stationary Poisson Model to Explain the Multi-Scaling of Network Flow Fluctuations

Yudong Chen, Li Li, Yi Zhang, Jianming Hu\*

(Dated: May 29, 2019)

## Abstract

In complex networks (systems) studies, the scaling phenomenon of flux usually refers to a certain power-law between the mean flux (activity)  $\langle F_i \rangle$  of the  $i$ th node (constituents) and the variance  $\sigma_i$  as  $\sigma_i \propto \langle F_i \rangle^\alpha$ . Though the scaling/multi-scaling laws are found to be prevalent in the natural and man-made network systems, our understanding of their origins still remains limited. In this paper, a non-stationary Poisson model is proposed to give a reasonable explanation of the non-universal scaling phenomena: the exponent  $\alpha$  varies between 1/2 and 1 with respect to the size of sampling time scale and the ratio of the internal/external driven forces of the systems. The non-universal  $\alpha$  values and their coexistence with long-range correlations are explained analytically and numerically. Experiments based on this model also accounts for the “crossover” and multi-scaling phenomena.

PACS numbers: 89.75.-k, 89.75.Da, 05.40.-a,

---

\*Department of Automation, Tsinghua University, Beijing 100084, P. R. China; Electronic address: li-li@mail.tsinghua.edu.cn

## I. INTRODUCTION

The studies of the complex networks have emerged and attracted increasing interests since the last decade [1], [2], [3]. Great works were devoted to the understanding of the network topologies and dynamic processes of network flows, which result in some significant achievements. However, there are still numerous interesting questions that remain to be thoroughly answered. One of them that will be emphasized in this paper is the origin of the fluctuations of networked flow.

To examine the collective behaviors of fluctuations over networks, Menezes and Barabasi proposed the so called scaling analysis to simultaneously describe the dynamics of a great number of network nodes by investigating the coupling between the average flux and fluctuations [4], [5], [6]. They found that in complex networks there is a characteristic coupling between the mean flux and variance of individual nodes as  $\sigma_i$  as  $\sigma_i \propto \langle F_i \rangle^\alpha$ . Such scaling law was found to hold in a wide range of aggregative systems. Moreover, analyses indicate that some important systems belong to either of two extreme universality classes. One class yields  $\alpha \approx 1/2$ , which means the external factors dominate system dynamics. Internet and microchip systems belong to this class. The other yields  $\alpha \approx 1$ , which indicates the internal dominance in the fluctuations. Highway traffic, river networks and the World Wide Web (of web pages and links) belong to this class. They believed that the value of  $\alpha$  indicates the dominance of either the system's internal collective dynamics or the changes in the external environments.

This interesting finding soon initiated the following studies. The multi-scaling phenomena are revealed to be more frequent in complex networks, e.g. stock market [7], [8], gene systems [9], software developments [11], download networks [10] and urban transportation networks [12]. In these systems, a rich variety of exponent  $\alpha$  from 1/2 to 1 can be seen, and its values heavily depend on the size of sampling time scale and the relative strength of the external driven forces. Some systems even exhibit the so called crossover behaviors (different groups/types of nodes in the same system possess different values of  $\alpha$ ) [8], [11], [13]. These phenomena are believed to reflect the competition between the external and internal forces, as well as the inhomogeneity of complex systems [8], [12], [14].

The scaling law attracts great interests due to its importance but has not been thoroughly explained yet. Several models have been proposed to reproduce the scaling laws [5], [6], [13],

[14], [15], [16], most of which are based on random walk or diffusive dynamics models. These models can link the network topologies and the associated dynamic processes of network flows. However, there are some shortcomings in the known models:

1. most models reproduce the scaling law only via numerical simulations and do not give explicit expressions of scaling relationship;
2. most models do not analytically account for the influence of sampling time scale and the ratio of the internal/external driven forces simultaneously;
3. some models cannot explain the broad range of  $\alpha$  from 1/2 to 1 or the crossover phenomena.

In view of these problems, a non-stationary Poisson model is proposed in [17], which can explain both analytically and numerically the transition of *alpha* from 1/2 to 1, as well as its dependence on sampling time scale and internal/external driven forces. However, it is assumed in [17] that the length of the jumping time interval of the non-stationary Poisson process equals to that of the sampling time window. Thus it cannot well explain some multi-scaling behaviors.

The purpose of this paper is to extend the model initialized in [17] and provide a more comprehensive study. To this end, the crossover and multi-scaling behavior are carefully discussed by studying the influence of sampling time scale. Results show that the non-universal  $\alpha$  values can be explained in a more unified and concise way.

## II. A NEW MODEL FOR THE SCALING OF NETWORK FLUCTUATIONS

### A. The Discrete-Modulated Poisson Process Model

Suppose the network system consists of  $N$  nodes, and the arriving flux  $f_i(t)$  of the  $i$ th node at the  $t$ th exogenous recording time window follows a non-stationary Poisson distribution such that

$$f_i^T(t) \propto P(\lambda_i(t)\tau), \quad \text{for } i = 1, \dots, N; \quad t = 1, \dots, T \quad (1)$$

where  $T$  is the number of the observed flux data points.

The time-variant arriving rate  $\lambda_i(t)$  is assumed to change as a jump process but remain constant with each endogenous time intervals  $\tau$  (the length of  $\tau$  is controlled by the process itself and is independent of exogenous recording time interval which is simplified as uniformly 1 here) as

$$\lambda_i(t) = k_i \lambda_j(\tau), \quad (j-1)\tau + 1 \leq t \leq j\tau \quad (2)$$

where  $k_i \lambda_j(\tau)$  denotes the value of the arrival rate of the  $i$ th node for the  $j$ th endogenous time interval,  $j = 1, \dots, T/\tau$ .  $k_i$  is the scale coefficient which controls the relative magnitude of flux on the  $i$ th node. If  $\lambda_j(\tau)$  describes the external force that drives all nodes simultaneously,  $k_i$  can be taken as its corresponding distribution on each node.

Moreover,  $\lambda_j(\tau)$  is assumed to change network-wide synchronously every  $\hat{\tau} = L \times \tau$  endogenous time intervals and only takes  $M$  values ( $L, M \in N$ ). The probability of  $\lambda_j(l)$  taking the  $m$ th value follows a discrete distribution

$$Pr(\lambda_j(l) = \lambda_m) = P_m, \quad \text{for } m = 1, \dots, M, \quad l = \hat{\tau}, 2\hat{\tau}, \dots, \left\lceil \frac{T}{\hat{\tau}} \right\rceil \hat{\tau} \quad (3)$$

where  $\sum_{m=1}^M P_m = 1$ . In the rest of this paper,  $\lambda_j(\tau)$  will be abbreviated as  $\lambda_j$  for simplicity.

The model above is a non-stationary (non-homogenous) Poisson process whose arriving rate  $\lambda_i(t)$  varies according to the discrete process Eq.(3). Therefore, it is called Discrete-modulated Poisson Process (DMPP). Indeed, DMPP can be viewed as a simplification of the well-known Markov-modulated Poisson Process (MMPP), which is shown to be versatile in modeling network traffic, such as Internet traffic [18], [19], [20]; because the discrete distribution Eq.(3) can be taken as the stationary distribution of a certain Markov Process.

Given a sampling window size  $\Delta t$  (time scale), the observed flux data time series for the  $i$ th node at the sampling time  $s$  can be written as

$$F_i^{\Delta t}(s) = \sum_{t=(s-1)\Delta t+1}^{s\Delta t} f_i(t), \quad \text{for } s = 1, \dots, T/\Delta t \quad (4)$$

To make it more clear, the subscript  $i$  denotes the index of the nodes,  $t$ ,  $j$  and  $s$  denote the indexes of the exogenous, endogenous and sampling time intervals respectively in the rest of this paper. And the capital letter  $F$  denotes the sampled/aggregated flow, while small letter  $f$  denotes the original flow. The words ‘‘internal/external’’ are only used to describe the driving forces on the systems; while the words ‘‘endogenous/exdogenous’’ are

only used to distinguish the time intervals of the process variation and our recordings. It should be pointed out that the symbols used in this paper may have different meanings in our previous paper [17].

If we assume the ergodicity of this model (in brief, the long-time behavior of the system matches its equilibrium behavior) as well as the long enough recording time ( $T \gg \Delta t, T \gg \hat{\tau} = L \times \tau$ ), the observed mean flux at node  $i$  can be estimated as

$$\begin{aligned}
\langle F_i^{\Delta t} \rangle &= \frac{1}{T/\Delta t} \sum_{s=1}^{T/\Delta t} F_i^{\Delta t}(s) \\
&= \frac{\Delta t}{T} \sum_{s=1}^{T/\Delta t} \sum_{t=(s-1)\Delta t+1}^{s\Delta t} f_i(t) \\
&= \frac{\Delta t}{T} \sum_{t=1}^T f_i(t) \\
&= \frac{\Delta t}{T} \sum_{j=1}^{T/\hat{\tau}} \sum_{t=(j-1)\hat{\tau}+1}^{j\hat{\tau}} f_i(t) \\
&= \frac{\Delta t}{T} \sum_{j=1}^{T/\hat{\tau}} k_i \lambda_j \hat{\tau} \\
&= k_i \Delta t \frac{1}{T/\hat{\tau}} \sum_{j=1}^{T/\hat{\tau}} \lambda_j \\
&= k_i \Delta t \langle \lambda \rangle
\end{aligned} \tag{5}$$

where  $\langle \lambda \rangle = \frac{1}{T/\hat{\tau}} \sum_{j=1}^{T/\hat{\tau}} \lambda_j$ .

To obtain the variance  $(\sigma_i^{\Delta t})^2$  of the flux, we need to distinguish two cases in terms of sampling window size  $\Delta t$ .

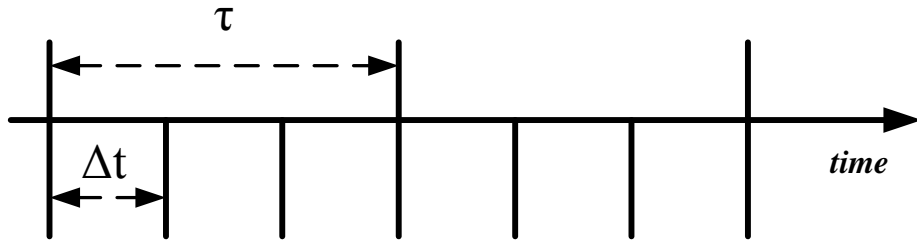


FIG. 1: Diagram of Case I), where  $\Delta t < \tau$ .

I)  $\Delta t \leq \hat{\tau}$ . Let's further assume that  $\hat{\tau} = \kappa \Delta t$ ,  $\kappa \in N$ , which indicates that the arrival

rate keeps constant in each sampling window. Note that the  $s$ th observed data satisfies  $F_i^{\Delta t}(s) \sim P(k_i \lambda_j \Delta t)$  for  $(j-1)\kappa + 1 \leq s \leq j\kappa$ , we have

$$\begin{aligned}
(\sigma_i^{\Delta t})^2 &= \frac{1}{T/\Delta t} \sum_{s=1}^{T/\Delta t} [F_i^{\Delta t}(s) - \langle F_i^{\Delta t} \rangle]^2 \\
&= \frac{\Delta t}{T} \sum_{s=1}^{T/\Delta t} [F_i^{\Delta t}(s)]^2 - \langle F_i^{\Delta t} \rangle^2 \\
&= \frac{\Delta t}{T} \sum_{j=1}^{T/\hat{\tau}} \sum_{s=(j-1)\kappa+1}^{j\kappa} [F_i^{\Delta t}(s)]^2 - (k_i \Delta t \langle \lambda \rangle)^2 \\
&= \frac{\Delta t}{T} \sum_{j=1}^{T/\hat{\tau}} \kappa \left[ \frac{1}{\kappa} \sum_{s=(j-1)\kappa+1}^{j\kappa} [F_i^{\Delta t}(s)]^2 \right] - (k_i \Delta t \langle \lambda \rangle)^2 \\
&= \frac{\Delta t}{T} \sum_{j=1}^{T/\hat{\tau}} \kappa [k_i \lambda_j \Delta t + (k_i \lambda_j \Delta t)^2] - (k_i \Delta t \langle \lambda \rangle)^2 \\
&= \frac{\kappa k_i (\Delta t)^2}{T} \sum_{j=1}^{T/\hat{\tau}} \lambda_j + \frac{\kappa (k_i)^2 (\Delta t)^3}{T} \sum_{j=1}^{T/\hat{\tau}} (\lambda_j)^2 - (k_i \Delta t \langle \lambda \rangle)^2 \\
&= k_i \Delta t \frac{\hat{\tau}}{T} \sum_{j=1}^{T/\hat{\tau}} \lambda_j + k_i^2 (\Delta t)^2 \frac{\hat{\tau}}{T} \sum_{j=1}^{T/\hat{\tau}} (\lambda_j)^2 - (k_i \Delta t \langle \lambda \rangle)^2 \\
&= k_i \Delta t \langle \lambda \rangle + k_i^2 (\Delta t)^2 [Var \lambda + \langle \lambda \rangle^2] - (k_i \Delta t \langle \lambda \rangle)^2 \\
&= k_i \Delta t \langle \lambda \rangle + k_i^2 (\Delta t)^2 Var \lambda \\
&= \langle F_i^{\Delta t} \rangle + \frac{Var \lambda}{\langle \lambda \rangle^2} \langle F_i^{\Delta t} \rangle^2
\end{aligned} \tag{6}$$

where  $Var \lambda = \frac{\hat{\tau}}{T} \sum_{j=1}^{T/\hat{\tau}} (\lambda_j - \langle \lambda \rangle)^2$ .

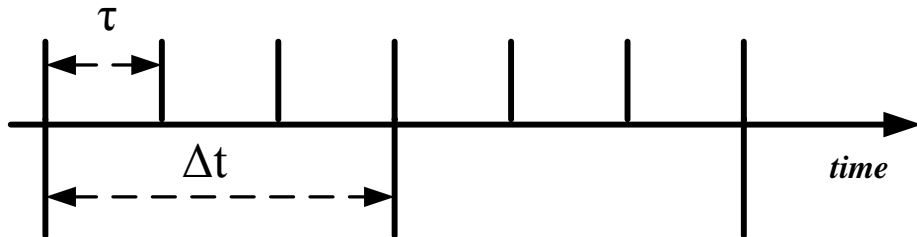


FIG. 2: Diagram of Case II), where  $\Delta t > \tau$ .

II)  $\Delta t > \hat{\tau}$ . Assume that  $\Delta t = \kappa \hat{\tau}$ ,  $\kappa \in N \setminus \{1\}$ , and note that

$$F_i^{\Delta t}(s) = \sum_{t=(s-1)\Delta t+1}^{s\Delta t} f_i(t) = \sum_{t=(j-1)\tau+1}^{j\tau} f_i(t) \sim P\left(\sum_{j=(s-1)\kappa+1}^{s\kappa} k_i \lambda_j \hat{\tau}\right) \quad (7)$$

and

$$\begin{aligned} (\sigma_i^{\Delta t})^2 &= \frac{1}{T/\Delta t} \sum_{s=1}^{T/\Delta t} [F_i^{\Delta t}(s) - \langle F_i^{\Delta t} \rangle]^2 \\ &= \frac{\Delta t}{T} \sum_{s=1}^{T/\Delta t} [F_i^{\Delta t}(s)]^2 - \langle F_i^{\Delta t} \rangle^2 \\ &= \frac{\Delta t}{T} \sum_{s=1}^{T/\Delta t} \left[ \sum_{j=(s-1)\kappa+1}^{s\kappa} \sum_{t=(j-1)\tau+1}^{j\tau} f_i(t) \right]^2 - \langle F_i^{\Delta t} \rangle^2 \\ &= \frac{\Delta t}{T} \sum_{s=1}^{T/\Delta t} \left[ \kappa \cdot \frac{1}{\kappa} \sum_{j=(s-1)\kappa+1}^{s\kappa} \left( \tau \cdot \frac{1}{\tau} \sum_{t=(j-1)\tau+1}^{j\tau} f_i(t) \right) \right]^2 - \langle F_i^{\Delta t} \rangle^2 \\ &= \frac{\Delta t}{T} \sum_{s=1}^{T/\Delta t} \left[ \kappa \cdot \frac{1}{\kappa} \sum_{j=(s-1)\kappa+1}^{s\kappa} \tau k_i \lambda_j \right]^2 - (k_i \Delta t \langle \lambda \rangle)^2 \\ &= \frac{\Delta t}{T} (k_i \kappa \tau)^2 \sum_{s=1}^{T/\Delta t} \left[ \frac{1}{\kappa} \sum_{j=(s-1)\kappa+1}^{s\kappa} \lambda_j \right]^2 - (k_i \Delta t \langle \lambda \rangle)^2 \end{aligned} \quad (8)$$

Let  $\Lambda_s = \frac{1}{\kappa} \sum_{j=(s-1)\kappa+1}^{s\kappa} \lambda_j$  denote the average of  $\lambda_j$  in the  $s$ th sampling window  $j \in [(s-1)\kappa+1, s\kappa]$ . Note that  $\langle \Lambda \rangle = \langle \lambda \rangle$ , Eq.(8) can be further simplified as

$$\begin{aligned} (\sigma_i^{\Delta t})^2 &= \frac{\Delta t}{T} (k_i \Delta t)^2 \sum_{s=1}^{T/\Delta t} (\Lambda_s)^2 - (k_i \Delta t)^2 \langle \Lambda \rangle^2 \\ &= (k_i \Delta t)^2 \text{Var} \Lambda \\ &= \frac{\text{Var} \Lambda}{\langle \lambda \rangle^2} \langle F_i^{\Delta t}(s) \rangle^2 \end{aligned} \quad (9)$$

where

$$\text{Var} \Lambda = \frac{1}{T/\Delta t} \sum_{s=1}^{T/\Delta t} (\Lambda_s - \langle \Lambda \rangle)^2 \quad (10)$$

For convenience, we rewrite Eq.(5), (6) and (9) in short as

$$\langle F_i^{\Delta t} \rangle = k_i \Delta t \cdot \langle \lambda \rangle \quad (11)$$

and

$$(\sigma_i^{\Delta t})^2 = \begin{cases} k_i \Delta t \langle \lambda \rangle + (k_i \Delta t)^2 \text{Var} \lambda = \langle F_i^{\Delta t} \rangle + \frac{\text{Var} \lambda}{\langle \lambda \rangle^2} \langle F_i^{\Delta t} \rangle^2, & \Delta t \leq \hat{\tau} \\ (k_i \Delta t)^2 \text{Var} \Lambda = \frac{\text{Var} \Lambda}{\langle \lambda \rangle^2} \langle F_i^{\Delta t} \rangle^2, & \Delta t > \hat{\tau} \end{cases} \quad (12)$$

It should be pointed out that we take weaker assumptions here instead of some more complicated cases in which  $\kappa$  is not a integer. However, the following studies show that the aforementioned assumption is already able to reproduce the empirical scaling phenomena that have been observed.

## B. The Scaling of Fluctuations of the DMPP Model

Based on Eq.(11)-(12), the scaling law of the proposed model can be analytically determined. Particularly, this sub-section discusses the following three issues that had been addressed in many previous works:

### 1) The Influence of the Competition of Internal/External Force

The time-variation of  $\lambda_j$  can be regarded as the result of external driven force, and thus the ratio  $\text{Var} \lambda / \langle \lambda \rangle$  (or  $\text{Var} \Lambda / \langle \lambda \rangle$ ) reflects its strength. If  $\Delta t \leq \tau$ , when the external force is weak, we get  $\text{Var} \lambda / \langle \lambda \rangle \ll 1$ . The second term in the r.h.s. of (12) can be omitted, and thus yields  $\alpha = 1/2$ . On the other hand, when the external force is strong  $\text{Var} \lambda / \langle \lambda \rangle \gg 1$ , the first term can be omitted which results in  $\alpha = 1$ . For intermediate values of  $\text{Var} \lambda / \langle \lambda \rangle$ ,  $\alpha$  ranges between 1/2 and 1. Similar results can be drawn for  $\alpha$  w.r.t  $\text{Var} \Lambda / \langle \lambda \rangle$ , if  $\Delta t > \tau$ .

### 2) The Influence of Sampling Window

For a sampling window  $\Delta t \ll 1/\langle \lambda \rangle$ , we can omit the second term in the r.h.s. of (12) which contain the quadratic form of  $\Delta t$ . Thus we have  $(\sigma_i^{\Delta t})^2 \sim \langle F_i^{\Delta t} \rangle$  and  $\alpha = 1/2$  [26]. For a sampling window  $\Delta t \gg 1/\langle \lambda \rangle$ , we can omit the first term in the r.h.s. of (12), and thus  $(\sigma_i^{\Delta t})^2 \sim \langle F_i^{\Delta t} \rangle^2$  and  $\alpha = 1$ . It is clear that  $\alpha$  lies between 1/2 and 1 for any intermediate value of  $\Delta t$ .

### 3) The Existence of Crossover Behavior

Similarly, for nodes with  $k_i \gg k_i^2$  (or equivalently  $k_i \ll 1$ ), the second term in the r.h.s. of (12) can be omitted and we get  $\alpha = 1/2$ . For nodes with  $k_i \ll k_i^2$  (or equivalently  $k_i \gg 1$ ), the first term in the r.h.s. of (12) is omitted and we have  $\alpha = 1$ . If the complex systems



consists of a broad range of  $k_i$  across nodes, it can be expected that different groups of nodes (subsystems with different  $k_i$  and  $\langle F_i^{\Delta t} \rangle$ ) scale with different exponents  $\alpha$ .

#### 4) The Coexistence with Long-Range Correlations

Besides scaling law, long-range correlation represents another kind power law between the variance and the sampling window size

$$\sigma_i(\Delta t) \propto \Delta t^{H(i)} \quad (13)$$

where  $H(t)$  denotes the well known Hurst exponent.

Investigations show that in some systems (i.e. stock markets), these two power-laws are found coexisted. To explain such phenomena, several models were developed. In [14], [21], [22], a random walker model was proposed, which states that the only possible way for these two power-laws to coexist, is when

$$\alpha(\Delta t) = \alpha^* + \gamma \log \Delta t, H(i) = H^* + \gamma \log \langle F_i \rangle \quad (14)$$

where the two slopes  $\gamma$  are interestingly the same for the two power-laws.

This conclusion agrees with the observations that the variation of sampling time window (aggregation time scale) has similar influence on two exponents  $\alpha(\Delta t)$  and  $H(i)$ . With the model proposed in this paper, we can provide a nice explanation for these phenomena. Based on (5), we can derive the coexistence of the two power laws directly. Moreover, based on (5) and (12), it is apparent that these two power laws has the same increasing slopes  $\gamma$  defined in (14).

### III. NUMERICAL EXPERIMENTS FOR THE MULTI-SCALING OF NETWORK FLUCTUATIONS

In this section, some numerical experiments are designed to give some impressive illustrations of the proposed model.

#### 1) The Influence of the Competition of Internal/External Force

In this third test, the corresponding parameters of the model are set as  $N = 20$ ,  $T = 100000$ ,  $M = 10$ ,  $\tau = 1$ ,  $L = 1$ ,  $\Delta t = 1$ .  $p_j = 1/10$  for  $j = 1, \dots, 10$ ,  $\lambda_j = [1, 2, 3, \dots, 10]$ . The ratio  $Var\lambda/\langle\lambda\rangle$  is controlled to vary from 0 to 200. The transition of  $\alpha$  from 1/2 to

1 w.r.t  $Var\lambda/\langle\lambda\rangle$  can be clearly observed from the obtained Fig.3. Similar results can be found that  $\Delta t > \tau$  cases and are thus omitted here.

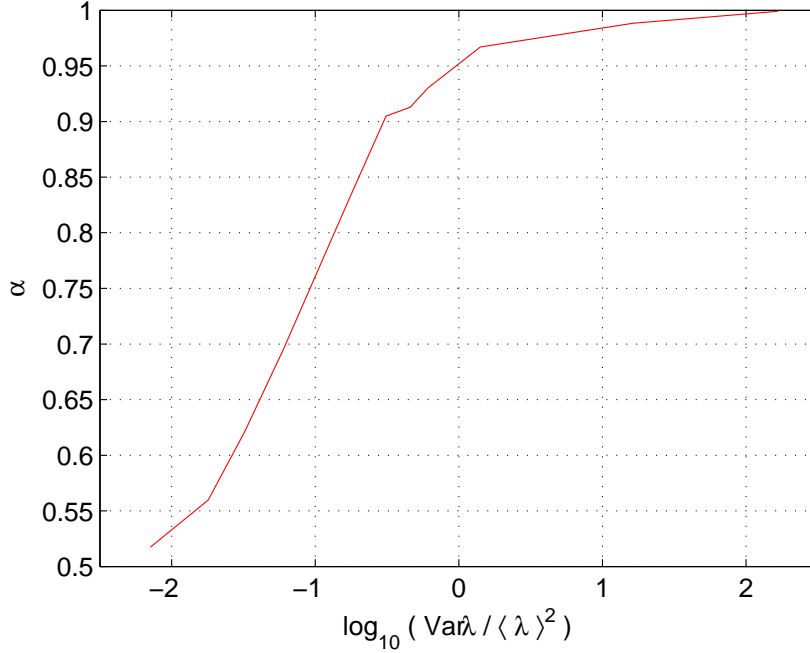


FIG. 3: An example of the transition behavior of  $\alpha$  w.r.t the competition of internal/external force reproduced by the proposed model.

## 2) The Influence of the Sampling Time Scale

In this second test, the corresponding parameters of the model are set as  $N = 20$ ,  $T = 1000000$ ,  $M = 2$ ,  $\tau = 1$ ,  $L = 10$ .  $p_j = 1/2$  for  $j = 1, 2$ ,  $\lambda_j = [0.8, 1.1]$ .  $k = [10, \dots, 20]$ . The sampling window size  $\Delta t = 1$  is controlled to vary from 1 to 15. The transition of  $\alpha$  from 0.6140 to 0.9036 w.r.t  $Var\lambda/\langle\lambda\rangle$  can be clearly observed from the obtained Fig.3.

## 3) The Existence of Crossover Behavior

In this third test, the corresponding parameters of the model are set as  $N = 20$ ,  $T = 100000$ ,  $M = 10$ ,  $\tau = 1$ ,  $L = 1$ ,  $\Delta t = 1$ .  $p_j = 1/10$  for  $j = 1, \dots, 10$ ,  $\lambda_j = [1, 2, 3, \dots, 10]$ .  $k = [0.5, 0.5^2, \dots, 0.5^8, 1, 2, 5, 5^2, \dots, 5^{10}]$ . The obtained Fig.5 shows a typical example of crossover behavior, in which the slopes of the two identified lines are 0.54 and 0.99, respectively.

## 4) The Existence of Multi-Scaling Behavior

The scaling law  $\sigma_i \sim \langle F_i^{\Delta t} \rangle^\alpha$  can be generalized to arbitrary  $q$ -th-order central moments as

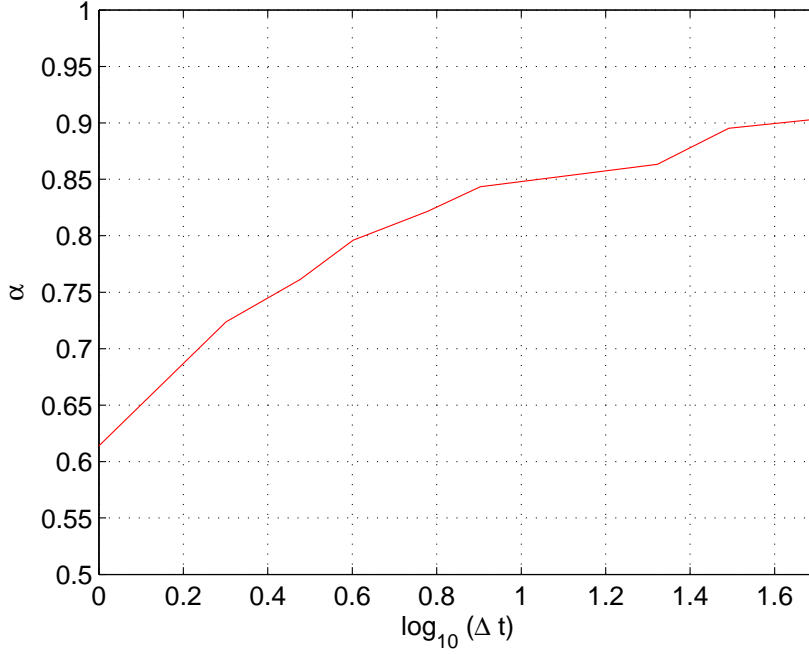


FIG. 4: An example of the transition behavior of  $\alpha$  w.r.t the sampling time scale reproduced by the proposed model.

$$\sigma_{i,q} = \langle |F_i^{\Delta t} - \langle F_i^{\Delta t} \rangle|^q \rangle \propto \langle F_i^{\Delta t} \rangle^{q\alpha(q)} \quad (15)$$

Generally, this multi-scaling law (i.e. a dependence of  $\alpha(q)$  on  $q$ ) is assumed to be related with the multi-fractality of time series [14]. And the model proposed here can easily produced multi-scaling phenomena.

In this fourth test, the corresponding parameters of the model are set as  $N = 20$ ,  $T = 10000$ ,  $M = 10$ ,  $\tau = 10$ ,  $L = 1$ .  $p_j = 1/10$  for  $j = 1, \dots, 10$ ,  $\lambda_j = [2, 3, \dots, 11]$ .  $k = [1, 2, \dots, 10]$ . Fig.(6) shows three  $q$ - $\alpha(q)$  plots for  $\Delta t = 1$ ,  $\Delta t = 10$  and  $\Delta t = 100$ , respectively. in which the multi-scaling phenomena can be clearly seen.

#### IV. CONCLUSION

A non-stationary Poisson model is introduced in this paper to explain the multi-scaling fluctuations in complex systems. We find that non-universal behavior is manifested not only in the scaling exponent  $\alpha$  different from the universal values  $1/2$  and  $1$ , but also in the scaling properties of the distribution functions. The influences of sampling time scale and

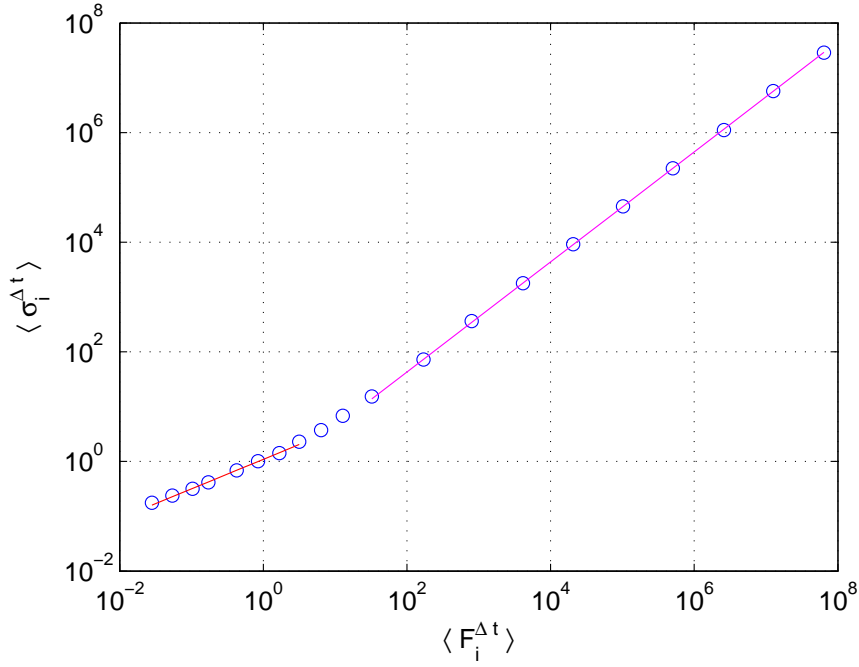


FIG. 5: An example of crossover behavior reproduced by the proposed model.

internal/ external force ratio are also naturally accounted for. The model is validated by simulations, and the behaviors of an urban transportation system are well reproduced.

These results show that the proposed model helps explain the mechanism of the collective dynamics of complex systems, and is suitable for the simulation of a broad range of systems. Barabasi’s view of distinguishing internal and external dynamics by the value of  $\alpha$  is proven to be helpful in our model, too. But it is meanwhile revealed that the influences of sampling time scale and inhomogeneous structure must be carefully considered before making any conclusion on the driving forces.

Our work also in a sense shed lights on the well-known debate whether Poisson models are applicable in modeling modern communication network systems [23], [24], [25]. The presented results support the following argument: the non-stationary Poisson process may still be useful in modeling such complex time-variant systems with complicated internal/external interactions and the resulting behaviors at different time-scales.

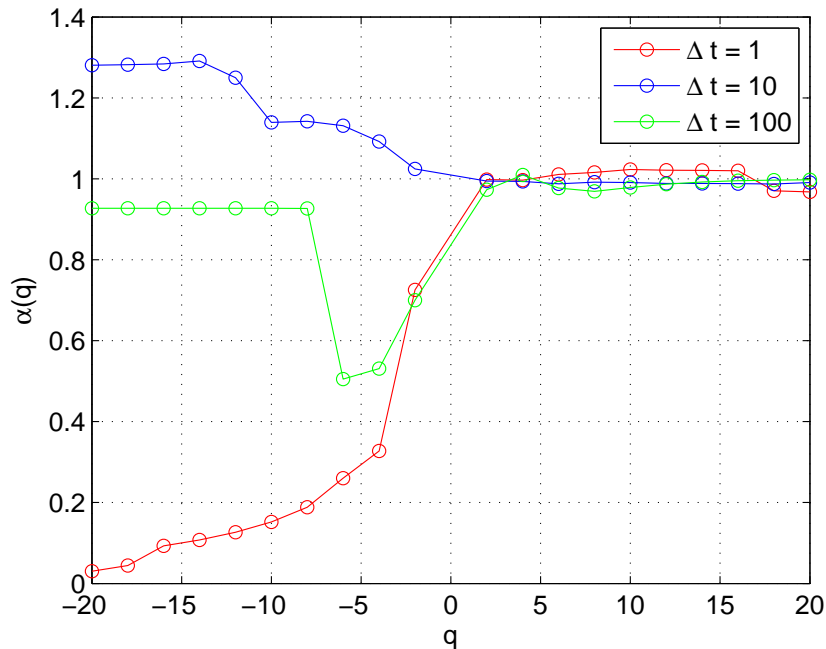


FIG. 6: An example of multi-scaling behavior reproduced by the proposed model.

### Acknowledgments

This work was supported in part by National Basic Research Program of China (973 Project) 2006CB705506, Hi-Tech Research and Development Program of China (863 Project) 2007AA11Z222, National Natural Science Foundations of China 60721003, 60774034.

- 
- [1] R. Albert, A.-L. Barabasi, *Rev. Mod. Phys.* **74**, 47 (2002).
  - [2] M. E. J. Newman, *SIAM Rev.* **45**, 167 (2003).
  - [3] S. Boccaletti, V. Latorab, Y. Morenod, M. Chavezf, D.-U. Hwanga, *Phys. Rep.* **424**, 175 (2006).
  - [4] M. A. de Menezes, A. L. Barabasi, *Phys. Rev. Lett.* **92**, 028701 (2004).
  - [5] M. A. de Menezes, A. L. Barabasi, *Phys. Rev. Lett.* **93**, 068701 (2004).
  - [6] Z. Eisler, J. Kertesz, S.-H. Yook, A. L. Barabasi, *Europhysics Lett.* **69**, 664 (2005).
  - [7] Z. Eisler and J. Kertesz, *Phys. Rev. E* **73**, 046109 (2006).

- [8] G. Raffaelli, M. Marsili, *J. Stat. Mech. Theory and Exp.* **08**, L08001 (2006).
- [9] J. C. Nacher, T. Ochiai, T. Akutsu, *Mod. Phys. Lett. B* **19**, 1169 (2005).
- [10] D.-D. Han, J.-G. Liu, Y.-G. Ma, *Chin. Phys. Lett.* **25**, 765 (2008).
- [11] S. Valverde, *Europhys. Lett.* **77**, 20002 (2007).
- [12] Y. Chen, L. Li, Y. Zhang, J. Hu, X. Jin, *Mod. Phys. Lett. B* **22**, 101 (2008).
- [13] B. Kujawski, B. Tadic and G. J. Rodgers, *New J. Phys.* **9**, 154 (2007).
- [14] Z. Eisler, J. Kertesz, *Phys. Rev. E* **71**, 057104 (2005).
- [15] J. Duch and A. Arenas, *Phys. Rev. Lett.* **96**, 218702 (2006).
- [16] J. Duch, A. Arenas, *Eur. Phys. J. - Spec. Top.* **143**, 253 (2007).
- [17] Y. Chen, L. Li, Y. Zhang, X. Jin, *Chinese Phys. Lett.* **22**, 101 (2008).
- [18] M. Rossiter, *Australian Telecommunication Research* **21**, 53 (1987).
- [19] W. Fischer and K. Meier-Hellstern, *Performance Evaluation* **18**, 149 (1992).
- [20] G. Bolch, S. Greiner, H. de Meer, K. S. Trivedi, H. de Meer, K. S. Trivedi, *Queueing Networks and Markov Chains: Modeling and Performance Evaluation with Computer Science Applications*, 2nd ed., (John Wiley and Sons, 2006).
- [21] Z. Eisler, J. Kertesz, *Phys. Rev. E* **73**, 046109 (2006).
- [22] Z. Eisler, J. Kertesz, in *Econophysics of Stock and other Markets*, A. Chatterjee, B. K. Chakrabarti, eds. Springer, Milan, 49, (2006).
- [23] V. Paxson and S. Floyd, *IEEE/ACM Transactions on Networking* **3**, 226 (1995).
- [24] J. Cao, S. C. William, D. Lin, X. S. Don, *ACM SIGMETRICS Performance Evaluation Review* **29**, 102 (2001)
- [25] T. Karagiannis, M. Molle, M. Faloutsos, and A. Broido, in *Proceedings of INFOCOM*, 2004.
- [26] As pointed out in [15], in the limit of infinitesimal sampling window such that  $\langle F_i^{\Delta t} \rangle \ll 1$ , we always recover  $\alpha = 1/2$  regardless the underlying arriving process.